Electric Power Systems Research 182 (2020) 106204

Contents lists available at ScienceDirect

Electric Power Systems Research

journal homepage: www.elsevier.com/locate/epsr

Probabilistic analysis of switching transients due to vacuum circuit breaker operation on wind turbine step-up transformers

Sajjad Ghasemi[a], Mehdi Allahbakhshi[a,*], Behzad Behdani[a], Mohsen Tajdinian[a], Marjan Popov[b]

[a] School of Electrical and Computer Engineering, Shiraz University, Shiraz, Iran
[b] Delft University of Technology, Faculty of EEMCS, Delft, Netherlands

ARTICLE INFO

Keywords:
Switching transients
Vacuum circuit breaker
Statistical transient
Restrikes

ABSTRACT

Vacuum circuit breaker operation causes transient overvoltages that may lead to severe damages to transformer insulation. Since the parameters affecting these overvoltages have stochastic nature, a statistical analysis may provide detailed insight into the overvoltages from the point of view of insulation coordination applications. In this paper, a statistical analysis of the overvoltage variations of the step-up transformer during vacuum circuit breaker operation is conducted. Some variables, including switching angle, current chopping, high-frequency current quenching capability, and wind turbine power, are assumed as random variables. Besides, some indicators representing the switching overvoltage characteristics such as the amplitude, the number of restrikes, and the rate of rise are extracted. By performing a probabilistic analysis, the destructiveness due to switching overvoltages on typical transformer insulation can be investigated. The sensitivity of different surge protective devices and their effectivities are also analyzed and statistically evaluated. The applied methodology is very useful because of the stochastic nature of the switching overvoltages. In this work, the impact of protective equipment on each of the overvoltage indicators is analyzed. It is also found that considering only the amplitudes of transient overvoltages is not enough to draw conclusions about the safety of the transformer when exposed to frequent switching surges.

1. Introduction

VCBs are commonly used in offshore wind farms due to their ability to eliminate high fault currents and their low maintenance costs. Due to wind speed variations, numerous switching actions (energization and de-energization) commonly occur in wind farms every day. VCB switching transients reach the step-up transformer through the short cable connected to the wind turbine.

In case, the amplitude of a switching transient voltage rises above the BIL; it can lead to transformer winding failures. Previous statistical studies related to VCB opening were only focused on the amplitude of transient overvoltages regardless of their rise times [1–4] However, some transformer failures due to VCB operations have indicated that the leading cause of the failure was the high du/dt [5]. Recently performed detailed research showed that due to fast transients and during resonance conditions, the voltages with high amplitudes are non-linearly distributed along the windings [6], and the high du/dt accelerates failure mechanisms because of high interturn overvoltages in the transformer windings; causing coil-to-coil failures in the top or in the middle of the winding.

Besides, the critical voltage of the transformer BIL remarkably decreases with the reduction of the rise time [7,8] and the amplitude [7] of the transient voltage applied. Moreover, the experimental studies confirm the effects of lightning impulses on oiled paper [9] and very fast transients on cast-resin insulation [10]. Accordingly, the rate of rise and the number of transient surges should be considered alongside their amplitude in a stochastic analysis in order to accurately assess the effects of the switching overvoltages on transformer insulation lifetime.

The characteristics of the transient overvoltages occurring due to VCB operation depend on various parameters. The current chopping phenomenon in VCBs being one of the key parameters that contribute to the reignition overvoltages. Experimental tests conducted in Ref. [11] however, showed the low dependency of this parameter on the operation instant.

Generally, the interruption of high-frequency currents is assumed after the first zero-crossing in most studies, yet nevertheless, the current zero-crossing has a stochastic behavior according to Ref. [12].

Another effective parameter which is important for the characteristics of VCB switching transient overvoltage applied to the step-up transformer is its loading condition. Studies conducted in Ref. [13]

* Corresponding author.
E-mail address: allahbakhshi@shirazu.ac.ir (M. Allahbakhshi).

https://doi.org/10.1016/j.epsr.2020.106204
Received 11 June 2019; Received in revised form 29 December 2019; Accepted 6 January 2020
Available online 18 January 2020

Nomenclature

Abbreviation

VCB	Vacuum circuit breaker
BIL	Basic insulation level
SPD	Surge protective device
CDF	Cumulative density function
EMT	Electromagnetic transient
FDQ	Finite difference quadrature
TACS	Transient analysis of control systems
PDF	Probability density function

showed that switching overvoltages significantly vary by transformer loading conditions. That is to say, the transformer insulation is most severely affected by overvoltages introduced by switching of the transformer during unloaded, lightly loaded, and inductive-loaded operation condition [14]. It is worth mentioning that for the cases of line-charging, cable-charging, and capacitor banks, the current switching has a capacitive nature [15]. However, the measurements conducted in Ref. [16] suggest that capacitive switching does not show to be damaging to the transformer windings. Therefore, only the effect of inductive loading has been investigated in this study.

Although some researchers have focused on the deterministic studies of VCB switching transients [13,17,18], since many parameters influence the overvoltage level, it is more realistic and accurate to consider particular random variables and perform a statistical approach. Recently, one study [19], accurately investigated the effects of different parameters such as stray elements (resistances, inductances, and capacitances) of VCBs, cable's lengths, dielectric strength rates and switching angles on the overvoltage indicators such as rate of rises of surges and the number of restrikes during VCB opening, considering the transformer loading to be constant. However, the authors have considered a small number of switching cases and also the level of current chopping has been considered constant.

Different SPDs such as arresters and RC snubbers are applied to protect the transformer from switching overvoltages. The deterministic experimental results in Ref. [20] show that the use of RC snubbers results in low probability of reignition occurrence, whilst phase to ground arresters only affect the amplitude of overvoltages. A recent study has indicated the feasibility of employment of a series inductance, i.e. a choke to decrease the rate of rise of switching transient voltages (du/dt) [21]. So far, there has been no comparison carried out between the effect of a choke or a snubber on other overvoltage indicators to find out the convenience of using chokes instead of snubbers.

This paper provides a statistical analysis of transformer stresses due to VCB operation in a typical offshore wind farm. The proposed probabilistic framework can quantitatively and precisely evaluate the switching transients. Through the proposed framework and by utilizing some switching indicators, the sensitivity and also the efficiency of applied SPDs are investigated.

To conduct this investigation, firstly, transient models of the components of a typical wind farm are discussed in this paper. Thereafter, the accuracy of applied models and the impact of SPDs during VCB operation are determined through simulation. In order to provide sufficient samples for the analysis, 3000 VCB switching operations considering random variables are carried out for each case. Random variables including switching-off/on angle, high-frequency current quenching capability, current chopping and wind turbine power are taken into consideration. Overvoltage indicators such as the number of the restrikes, voltage variations during restrikes, the rate of rise of overvoltages are adopted. CDFs of overvoltage indicators are generated for each SPD employment condition. Furthermore, the results of different SPDs utilization strategy are compared to examine the

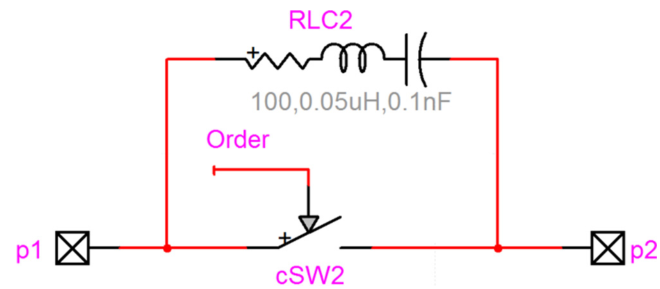

Fig. 1. VCB opening model in EMTP-RV.

implications of their utilization in the case study. Transformer failure associated with switching transients is evaluated by comparing the generated overvoltages to the critical overvoltages adopted according to existing standards as reported in Ref. [22].

2. System modelling

For the sake of sufficient accuracy, a user-defined wide band modelling of system components should necessarily be used for EMT-type studies [17]. The applied modeling approach is according to Ref. [12].

2.1. VCB modelling

Each phase of the circuit breaker model is represented by a controlled-switch, as shown in Fig.1. The controlled-switch operates according to the flowchart described in Ref. [23]. The series R, L and C elements connected in parallel to the ideal interrupter represent the stray parameters of VCB.

The withstand characteristic of the gap distance has a stochastic behavior. Experiment results in Ref. [24] show that the gap distance voltage at the first several millimeters of contacts separation can be first expressed as follows:

$$U_B = A(t - t_0) + B \tag{1}$$

where t_0 is the contact opening instant, B is the dielectric strength shortly after the contact poles are separated, and A is the opening speed. Due to the lack of measurements, the characteristics from Ref. [18] are applied.

The arc current during VCB opening is eliminated before the natural zero causing the current to chop. The level of current chopping in modern VCBs varies between 3 and 6 amperes. The highest current frequency that the breaker can interrupt at a current zero-crossing is depicted by its critical di/dt current derivative. A breaker's critical di/dt can be modeled statistically, varying between 100–600 A/μs [12]. An estimation for the mean value of di/dt can be calculated according to Eq. (2).

$$\frac{di}{dt} = C(t - t_0) + D \tag{2}$$

C and D constant are given in Table 1.

The algorithm that controls the effect of closing the VCB contacts is similar to that of opening, and the difference is that there is no current chopping and the dielectric withstand characteristic gradually decreases. The VCB parameters are considered according to Table 1.

Table 1
VCB parameters.

U_b, $\frac{di}{dt}$	$A\,[v/s]$	$B\,[v]$	$C\,[A/s^2]$	$D\,[A/s]$
Opening [25]	1.3×10^7	0.69×10^3	0.32×10^{12}	155×10^6
Closing	2×10^7	0	0	350×10^6

2.2. Test layout

Since the generated overvoltages and the design of SPDs in each system is unique, the simulation results of a complete wind farm cannot be used for another system. Therefore, a simplified layout consisting of a wind turbine connected to a network as a case study was selected, as shown in Fig. 2. The modeling of the wind turbine is realized by making use of the approach published in Ref. [10]; the inductor with the value proportional to the wind turbine's power is L = 0.318 mH. A 630 kVA, 24 kV/0.24 kV (Z_k = 6%) transformer with Y-Y grounded neutral connection is used as a step-up transformer, and the effect of saturation is not taken into account. The stray capacitances of transformer windings corresponding to capacitances between HV winding and ground, LV winding and ground, and HV and LV windings are C_H = 1 nF, C_L = 3.1 nF and $C_{L\text{-}H}$ = 3 nF, respectively. The VCB is connected to the transformer through an 80-meter cable (3 × 95 mm^2) and an FDQ model for the cable is used.

3. Surge protective device

3.1. Surge arrester

For the study of the effects of surge arresters on switching overvoltages, a simplified model is used, as shown in Fig. 3. The surge arrester's continuous operating voltage is selected according to IEC 60099-5, and the rated voltage of the surge arrester is $U_r = 1.25{\cdot}U_{c,min}$ [26]. The considered V-I characteristic of a 21 kV surge arrester according to the actual data [27] is presented in Table 2.

The values 0.200478 µH and 0.60143 µH; obtained from Eqs (3) and (4) are set to L_o and L_1 respectively. R = 1 MΩ is set according to Ref. [28].

$$L_0 = \frac{1}{12}.\frac{U_{r1/T2} - U_{r8/T2}}{U_{r8/T2}} \tag{3}$$

$$L_1 = \frac{1}{4}.\frac{U_{r1/T2} - U_{r8/T2}}{U_{r8/T2}} \tag{4}$$

In Figs. 4 and 5, the adopted phase voltages, with and without phase-to-ground arresters, are shown together. Fig. 5 shows the magnification of Fig. 4 in the time domain. The results express the arrester limits and the restrikes with amplitudes higher than approximately 50 kV (2 PU).

3.2. RC snubber

The snubber circuit consists of a surge capacitor connected in series to a damping resistor. This SPD reduces the steepness of surges. RC snubber is connected in parallel to the transformer terminals. The value of the resistance is normally chosen between 5–50 Ω [15]. The capacitance value is normally between 0.1–0.5 µF. The values C = 0.1 µF, R = 10 Ω are considered for this simulation. Fig. 6 and Fig. 7 show the effect of using an RC snubber on opening and closing transients of VCB, respectively. With the RC snubber implemented, there are only 2 restrikes occurred, which shows the prevention in the occurrence of repetitive overvoltages. RC snubbers provide excellent protection; however, they also occupy a lot of space and need regular periodic maintenances in order to make sure of their functionality. Other setbacks for RC snubbers are their heaviness and high costs and additionally, the injection of high amounts of reactive power into the

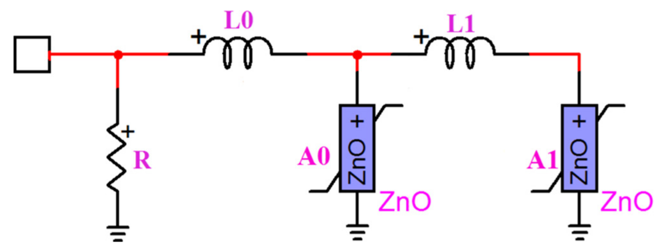

Fig. 3. Simplified surge arrester model.

Table 2
21 kV metal oxide surge arrester [27].

Wave 1/5 µs					U_r = 26.3 kV
	10		5	I [kA]	d = 387 mm
	70.4		66.5	V [kV]	n = 1
Wave 8/20 µs					
10	5	2.5	1	I [kA]	
64.5	60.9	58.1	54.9	V [kV]	
Wave 30/60 µs					
0.5	0.24	0.125		I [kA]	
51.6	49.7	47.8		V [kV]	

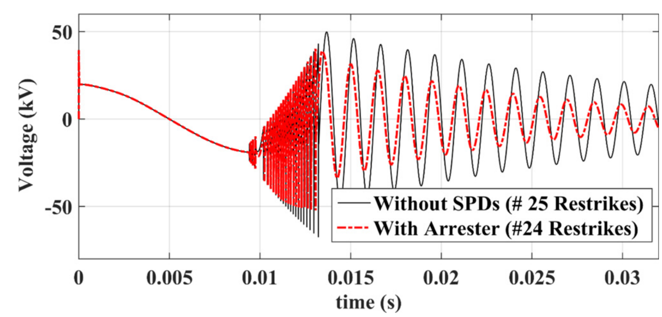

Fig. 4. Transformer voltage with and without surge arrester.

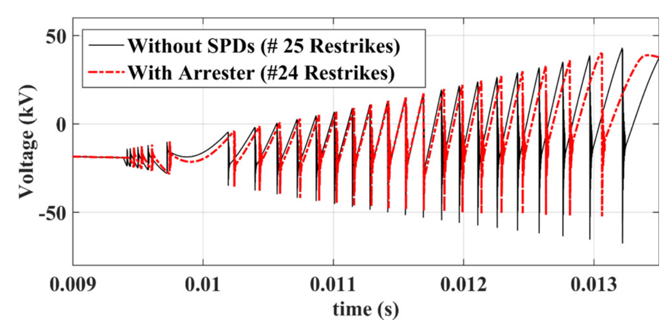

Fig. 5. Transformer voltage with and without arrester (magnified in time).

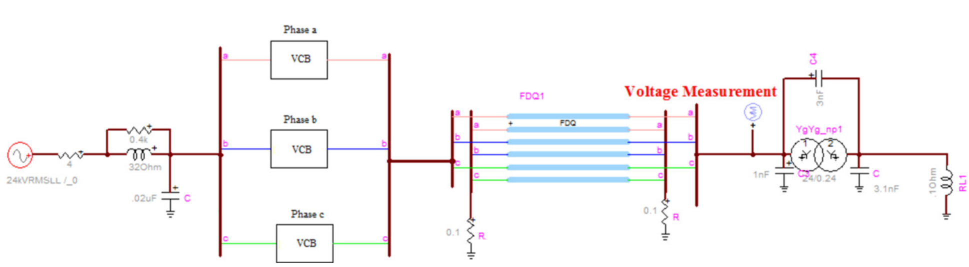

Fig. 2. EMTP-RV wind turbine power network model used for simulation.

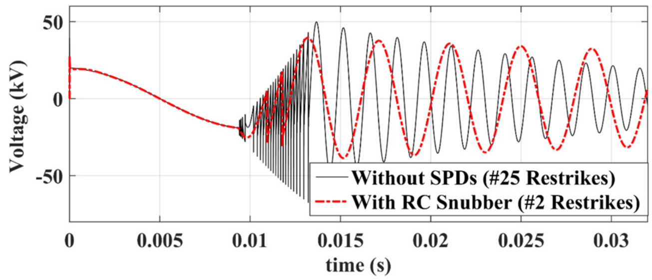

Fig. 6. Transformer voltage with and without RC snubber for VCB opening.

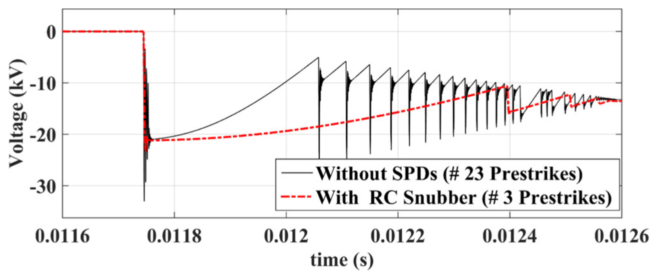

Fig. 7. Transformer voltage with and without RC snubber for VCB closing (magnified in time).

network and thus reduction of the power factor due to their high capacitance.

3.3. Choke (series inductance)

A choke is a device that consists of an inductance at the instant of switching. The connected cable goes through the choke, creating a magnetic couple with it. It acts as a low-pass filter, showing a low impedance in power frequency and applying a large impedance to the circuit at high frequencies [21]. The secondary winding of the choke is connected to a damping resistor, as shown in Fig. 8.

Literature [21] proposes a choke model which is a linear inductance in parallel with a resistance. The values 40 μH and 50 Ω are considered for the inductance and resistance, respectively. The effect of the choke on the VCB opening transients is shown in Fig. 9 and Fig. 10. The results show that the choke reduces the amplitudes of the transients during restrikes. It also eliminates high-frequency transients and reduces the slope (du/dt) of the restrikes, as depicted in Fig. 11.

4. Stochastic analysis

Practically, wind turbine switching has a stochastic nature, and therefore, the effectiveness of protective devices must be analyzed statistically. The statistical analysis has been performed on the VCB opening and closing actions to derive the distribution of peak values and the rate of rise of the generated transient overvoltages.

4.1. Random variables

As discussed in Ref. [19], many parameters such as the switching angle, the cable lengths between VCB and the transformer, the VCB parameters, and the VCB leakage parameters affect the VCB overvoltage opening. In the following, the parameters considered to be random in this study are introduced.

4.1.1. Switching-off/on angle

Generally, the overvoltage indicators highly depend on the voltage angle at which the VCB closes or opens. When the VCB opens/closes at the voltage peak, it experiences high stress. The switching-off/on angle is considered to be uniformly distributed.

4.1.2. Current chopping

The considerations for current chopping in this study are adopted from the experimental measurements in Ref. [11]. Therefore, current chopping has been assumed as a random variable with a log-normal PDF, and the values distributed between 3 to 6 A.

4.1.3. High-frequency current quenching capability

According to the experimental studies in Ref. [12], the high-frequency current quenching capability of the VCB is considered to be normally distributed within a 300–600 A/μs interval.

4.1.4. Wind turbine power

When analyzing a wind farm transformer switching, its power variations should be taken into account.

The generated power ($\bar{P}_w$) by a wind turbine is obtained according to Eq. (5) [29]. Where P_w represents the power output of the wind turbine as a function of the wind speed, and $f(u)$ describes the probability density function of the wind speed, which is usually modeled by making use of the Weibull distribution [30,31].

$$\bar{P}_w = \int_0^\infty P_w(u) f(u) du \tag{5}$$

In this study, power variations are considered to have a Weibull distribution with the parameters: shape factor = 2 and scale factor = 0.4.

4.2. Implementation of linking EMTP-RV to MATLAB

There are two methods for performing statistical analysis using EMTP [32]. One way is the internal programming as it is done in [2]. The other way, which is applied in this paper, is to link EMTP externally to an algorithm. The first method is applied by the use of EMTP TACS module. The second method allows calling EMTP-RV externally from a MATLAB M-File. The advantage of this method is the increase in computational speed and at the same time having access to the simulation results in a matrix form in the MATLAB environment. The procedure is conducted according to the flowchart in Fig. 12. The linking method is described in detail in Ref. [32]. In the first step, random variables are specified, and then, data vectors with the size of the Monte Carlo sample are generated for each random variable according to its distribution. For each Monte Carlo simulation, a set of random data is applied to the EMTP circuit, and the program is run. Simulation data is saved in a MATLAB M-File. The voltage measurement is done on the breaker side of the transformer, and later on, the overvoltage indicators are derived from each Monte Carlo simulation data. All simulations are performed in EMTP-RV software using a PC with an Intel Core i5 2.8 GHz processor and 8 GB RAM. Each simulation is done with a 50 ns time step, and the simulation time of 35 ms. Performing each Monte Carlo case with 3000 simulations using this PC takes approximately 24 h.

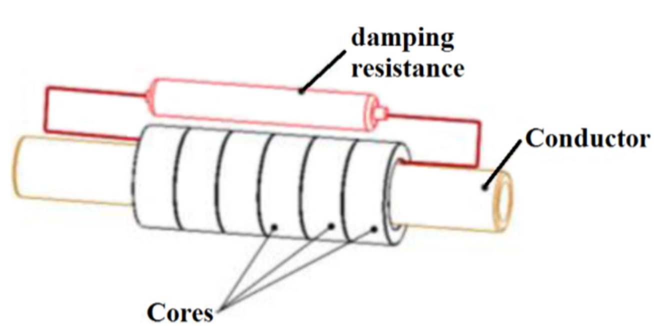

Fig. 8. Choke location around the cable [21].

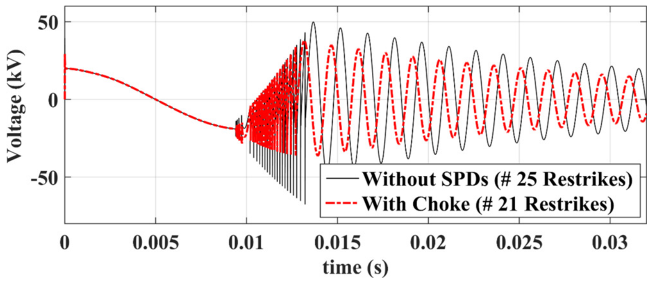

Fig. 9. Transformer voltage with and without a choke.

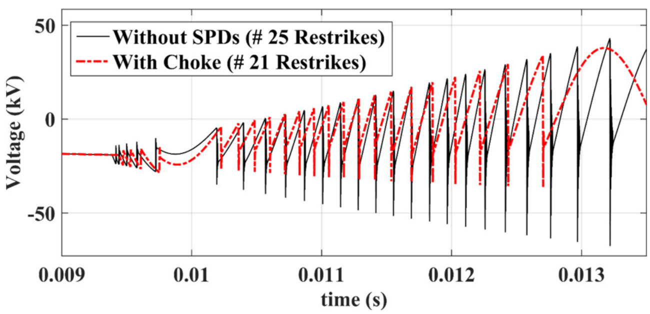

Fig. 10. Transformer voltage with and without a choke (increased time scale).

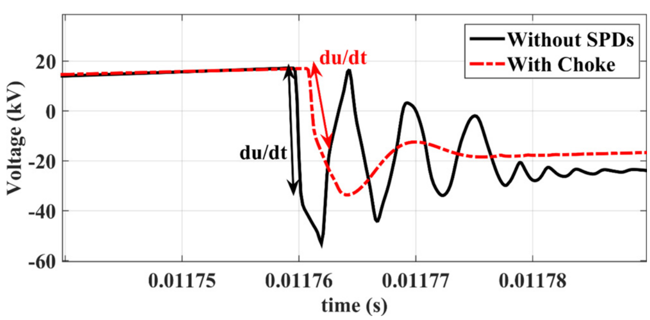

Fig. 11. The influence of the choke on the rate of rise of restrikes.

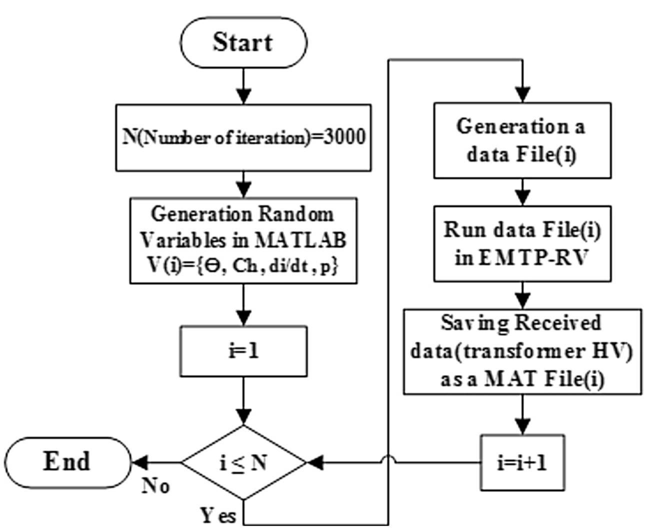

Fig. 12. EMTP-RV link to MATLAB flowchart.

4.3. Measurement of overvoltage indicators

The overvoltage indicators for each simulation are analyzed using the saved MATLAB M-File. Fig. 13 shows the measured voltage of the HV side of the transformer for one simulation as an example. The random variables for this example are considered $t_{trip} = 9$ ms, $I_{chopping} = 5.2$ A, and 20% for switching angle, current chopping, and power output are respectively shown in Fig. 13 where three major restrikes occurred in this example. Restrike regions in υ, and their number were obtained by defining a threshold value for fast data changes.

The restrikes are detected when a sudden voltage variation takes place. Voltage variation during a restrike is calculated through $DV = |V_{max} - V_{min}|$, as shown in Fig.14.

The rate of voltage variation, i.e. du/dt during a restrike is calculated through dividing the amount of voltage variation by its duration according to Eq. (6). The rise time ($t_{max} - t_{min}$) and the voltage variation are calculated as shown in Fig. 14.

$$\frac{du}{dt} = \left(\frac{U_{\max} - U_{\min}}{t_{\max} - t_{\min}}\right)_{5\%-75\%} \tag{6}$$

4.4. Analysis

4.4.1. VCB opening

Basically, a restrike is composed of three parts

1 The dielectric breakdown (arc ignition).
2 Current chopping (arc interruption).
3 Virtual current chopping.

The energy stored after the circuit breaker is opened is divided into two categories of energy, the electric energy (7) stored by the voltage in the breaker side capacitor and the magnetic energy (8) stored by the current in the load-side inductance [25].

$$W_{elec} = \frac{1}{2} C_T V_T^2 \tag{7}$$

$$W_{mag} = \frac{1}{2} L_T i_{Chop}^2 \tag{8}$$

The RC snubbers store energy in the system by creating a capacitive current path $\left(i_T - c\frac{dv}{dt}\right)$, whilst chokes actually reduce the steepness of the restrikes by creating a voltage drop $\left(v_T - l\frac{di}{dt}\right)$ [Fig. 15].

The distinguishing feature of VCBs from other types of breakers is that they forcibly eliminate the generated arc between their contact poles. The results in high current chopping levels in VCBs. Arc interruption does take place in other Breakers, too [5]. To better clarify the parameters involved in transients due to VCB opening, a scatter-plot of 3000 VCB opening for each case, showing the dependency of the voltage variation of each restrike (DV) to its rate (du/dt) has been developed as illustrated in Fig. 16.

The plotted data from each case except non-chopping VCB in Fig. 16 is subdivided into two branches. The branch specified by number (1) corresponds to dielectric breakdown; having higher variation rates, and the branch specified by number (2) corresponds to the current chopping; having higher amplitudes. Fig. 16 explicitly demonstrates the effectiveness of SPDs. One can well observe that the implementation of surge arresters –as expected- only limits the amplitude of restrike surges. It has only been capable of restricting 8% of the restrikes.

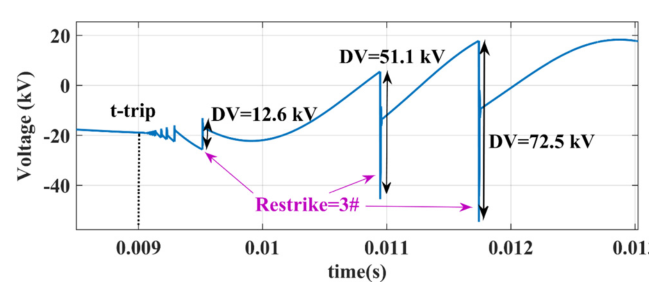

Fig. 13. Waveform of the high voltage side of the transformer.

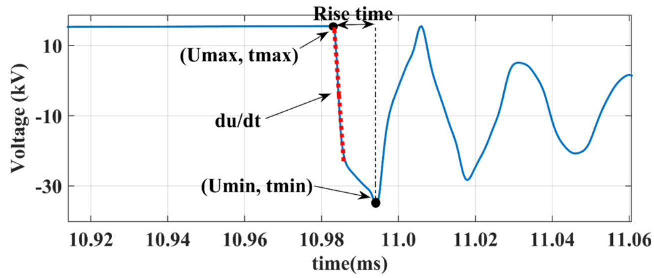

Fig. 14. Definition of du/dt for every strike.

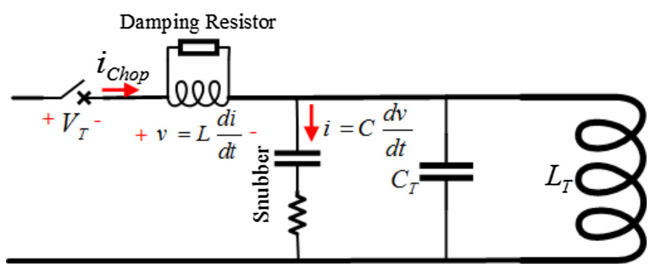

Fig. 15. Equivalent circuit of the breaker side.

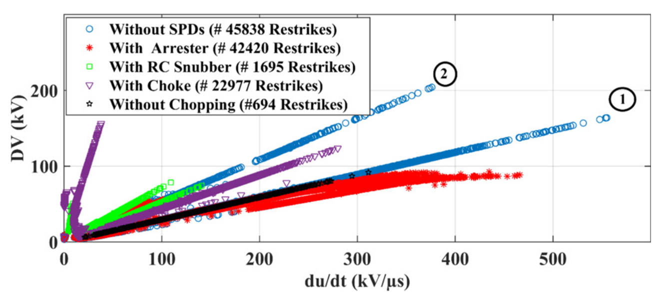

Fig. 16. Scatter plot diagrams of recorded restrikes.

The RC snubber, on the other hand, has shown better performance of reducing the number of restrikes with 96% of effectiveness. It can be seen in Fig. 16 that the RC snubber has also been able to limit both the rates and the amplitudes of the restriking voltage variations. The implementation of the choke reduces the number of restrikes by 49%. However, it is not able to reduce the high rates of voltage variations caused by the dielectric breakdown and also the high magnitude of voltage variations caused by current chopping very well.

Transformer sensitivity to surges can be charted in curves of acceptable voltage peak amplitude versus rise time [22] as shown in Fig. 17. NEMA, IEC and IEEE standards are for motors. Dashed line curve represents the proposed curve of literature [22] for the implementation of phase-ground surge arresters in transformer terminals. The implementation of a choke does not adequately protect the transformer, while a surge arrester provides a merely acceptable protection for the transformer. The RC snubber has shown to have the best performance in providing protection against surges. One can observe in Fig. 17 that there are also dangerous restrikes in the case of a non-chopping breaker. This means that dangerous restrikes may occur in VCBs with low current chopping levels too.

For the sake of statistical analysis, CDFs of the overvoltage indexes are plotted. From the CDFs, as shown in Fig. 18, it is clearly evident that the non-chopping breaker has generated fewer high amplitude restrikes compared to the chopping type. RC snubber had the best performance in limiting the amplitude of surges (90% of restrikes has 1.8 PU amplitude), and the chokes, on contrary, could not well reduce the amplitude of overvoltages. The CDF of restrikes' amplitude in non SPD implemented case (Fig. 18), shows only 0.36% of the overvoltages violate the BIL of the transformer insulation (125 kV = 5 PU), however, the previous evaluation of the non SPD implemented case with the proposed curve of the literature for transformers shows a much higher percentage of 11% hazardous restrikes (Fig. 17). Accordingly, it is totally negligent just to consider the overvoltage amplitudes without the assessment of their rise time. It should be noted this conclusion may vary for another case due to different parameters. The leakage capacitances for dry transformers is ten times lower than oiled transformers [22]. Using dry transformer and a 180 m cable can change the rise time and the number of restrikes very much as shown in Fig. 19.

The CDFs of the numbers of restrikes per VCB operation are shown in Fig. 20. The number of restrikes is considerably decreased in the CDFs of the non-chopping breaker and the case with RC snubber.

It can be concluded that the current chopping has a direct effect on restrike numbers. The implementation of a RC snubber could decrease the number of restrikes per opening by nearly 60%. The RC snubbers, as mentioned before, provide a current path for the chopped current of the VCB, and therefore it is very successful in reducing the number of restrikes. On the other hand, a choke basically affects the voltage of the surges and does not totally have an impact on the number of restrikes. As concluded in Fig.20 employing the choke alone will not effectively reduce the range of dangerous restrikes, and it just increases the slope of surges. As a result, in order to reduce the range of overvoltages, it is necessary to employ the choke in combination with the arrester.

The combined effect of the arrester and the choke (L = 40 μH) with different resistance values on restrikes is shown in Fig. 21. As it is evident, by increasing the value of the resistance above 50 ohms, an increase in rise time takes place. Almost all restrikes originated from different combinations of the arrester and the choke overlapped each other. This combination has significant poor performance in reducing the number of restrikes. Therefore, further increase in resistance does not change the value of the rise time. This finding coincides with the conclusion in Ref. [14]. It should be noted that the use of high resistance values can show little effect on the reduce of restrike numbers. Therefore, the best value for the choke can be the value close to the impedance characteristic of the cable.

4.4.2. VCB closing

Fig. 22 shows the scatter diagram of the recorded prestrikes of 3000 VCB closings for each case. The recorded number of prestrikes is observed to be lower than the number of restrikes. The reason is that there is no current chopping during the closing operation. An interesting observation here is that a choke shows a better performance in VCB closing than the opening of it. The reason for this event can be sought in the physics of the prestrikes. Prestrikes arise from the dielectric breakdown between the contact poles of the VCB and a voltage limitation –what a choke does- can well limit this phenomenon. The implementation of a choke prevented 77% of the prestrikes. Another fact is the inefficiency of surge arresters for limiting the number of prestrikes (just 2.2%) due to their inactivity for low amplitudes of

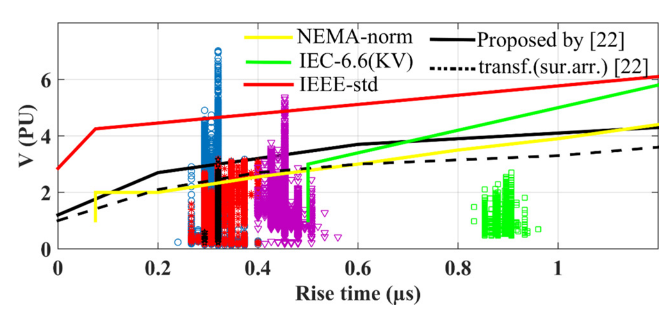

Fig. 17. Comparison of restrikes with different standard (color: blue circle = without SPD.
red star = with arrester, green square = with snubber and purple triangle = with choke)

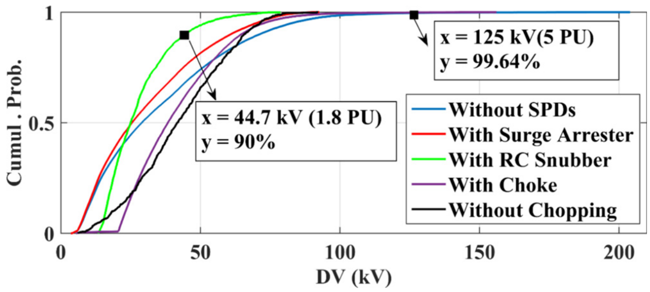

Fig. 18. CDFs of step changes of voltage (DV) during restrikes.

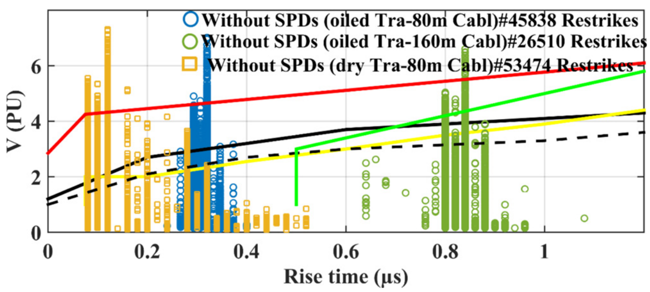

Fig. 19. Comparison of restrikes with different system parameters.

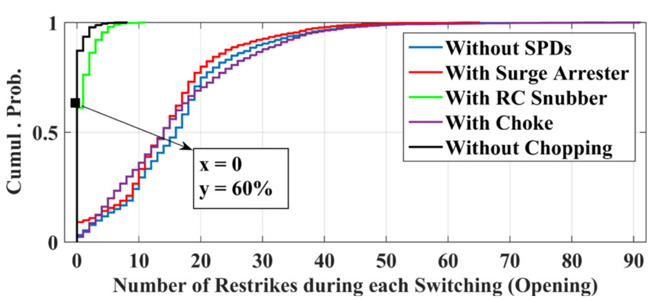

Fig. 20. CDFs of number of restrikes per opening operation.

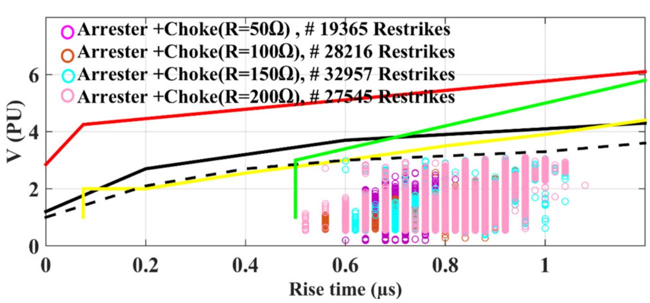

Fig. 21. The effect of different combination of choke and arrester on restrikes.

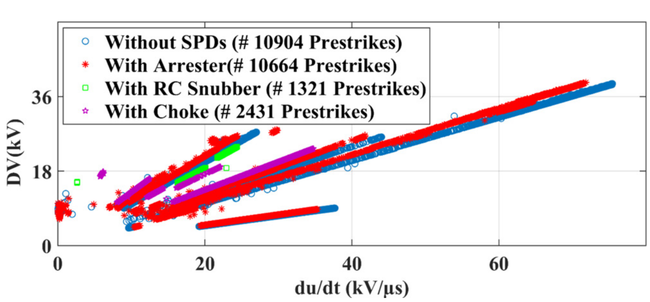

Fig. 22. Scatter plot diagrams of recorded prestrikes.

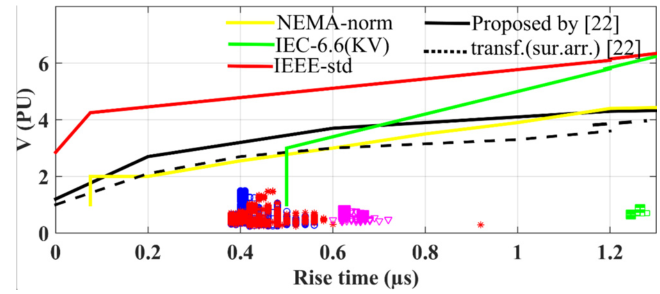

Fig. 23. Comparison of prestrikes with different standard (color: blue circle = without SPD, red star = with arrester, green square = with snubber and purple triangle = with choke).

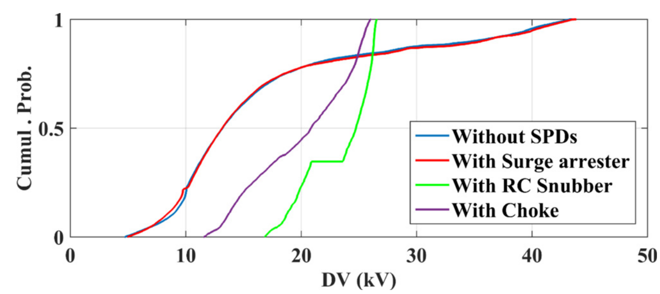

Fig. 24. CDFs of step changes of voltage (DV) during prestrikes.

prestrikes. RC snubbers again had the best impact in limiting the number of prestrikes (88%) among the SPDs.

Prestrikes, in comparison to restrikes have been observed to have greater rise times and lower amplitudes. Hence, none of the occurred prestrikes violates the proposed curve of lit. [22], as shown in Fig. 23. This observation is inconsistent with lit. [18] That mentions VCB closing prestrikes are not much of a problem for transformer insulation.

CFDs of the prestrike amplitudes are shown in Fig. 24. It is clear that no surges with the amplitude higher than the BIL of the transformer insulation have occurred. The CDF of the case of surge arrester implementation almost matches the CDF of the case with no SPDs. This is because of the amplitudes of the surges being lower than the protection level of surge arresters.

An interesting observation here is that the maximum amplitude of the occurred surges in the case of choke implementation is lower than that of a RC snubber implementation case. Fig. 25 shows the CDFs with the number of occurred prestrikes per VCB closing. Surge arresters have obviously shown to have a little impact on limiting the number of prestrikes. A RC snubber has managed to approximately limit the number of prestrikes to 3 prestrikes per closing. Choke implementation has also shown to have an excellent performance of limiting the number of prestrikes to 5 prestrikes in 96.53% of the VCB closings.

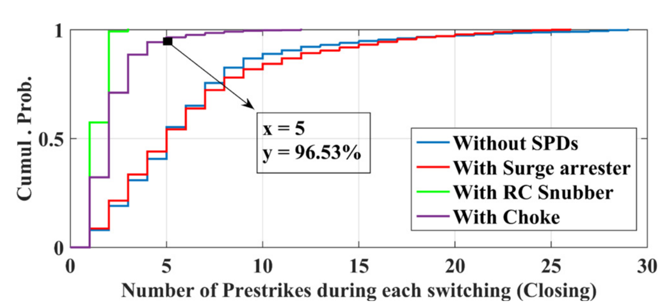

Fig. 25. CDFs of number of prestrikes per closing operation.

5. Conclusion

A statistical investigation has been conducted to analyze the switching surges due to VCB operation in a simplified offshore farm. Due to load parameters and equipment interactions, switching overvoltages in each system is unique [33] and switching overvoltages show highly stochastic behavior as many parameters influence the overvoltage in a unique system. Therefore, the applied methodology can help in the evaluation of overvoltage levels for a particular case and as it considers several stochastic variables in a particular case, which are essential for finding a solution to protect the transformer and the insulation. Concentrating on the wind speed as an influential random variable in wind turbine, it has been concluded that the quality of this statistical analysis has become more comprehensive. Moreover, it has been shown that the assessment of probabilistic insulation coordination by just considering the amplitudes of the surges is not sufficient. Therefore, the rate of rise of the overvoltages and the number of strikes should be considered for the determination of SPDs and the insulation level. The different cumulative distributions extracted from the stochastic analysis of switching transients in a unique system can be used for the estimation of transformer failure.

The steepness of switching transients caused by VCB closing was up to 5 times the steepness of opening overvoltages and the rise time of voltage surges due to VCB opening was approximately 0.75 the rise time of closing overvoltages. This shows that the current chopping may cause more effects on the amplitude of the overvoltages and the system parameters affecting the rise time of the overvoltages. Hence, the little difference in the rise time is due to the difference between the opening and the closing speed of the circuit breaker.

VCB prestrikes do not affect the insulation of the studied case. The SPD will be mandatory when only the number of prestrikes are concerned, and the choke is enough to use. About 89% of restrikes and 97.8% of prestrikes do not violate the BIL of the transformer in this circuit, which indicates that the effect of the arrester on the reduction of overvoltages is negligible. The implementation of the choke could not provide appropriate protection from overvoltage that results from current chopping. The impact of the choke on reducing the number of restrikes is approximately 49%, but its ability to limit the overvoltage amplitude is not reliable. It has been shown that the chokes make a significant impact on the number and the rise time of the prestrikes. RC snubbers provide the best performance in reducing the number, the amplitudes, and the rates of rise of the restrikes for both closing and opening operations, however, they are too expensive and hard to manage. In some cases, the available space for an RC snubber is intensely limited [5] because the snubber should be connected to the transformer terminal [34]. Therefore, it is proposed to use a surge arrester and a choke together to provide sufficient protection against a high rate of rise and severe reignitions, as the arrester limits the overvoltages and the choke decreases the severity of the restrikes.

Author contributions

Sajjad Ghasemi:
Conceived and designed the analysis
Collected the data
Contributed data or analysis tools
Performed the analysis
Wrote the paper
Mehdi Allahbakhshi:
Conceived and designed the analysis
Wrote the paper
Other contribution
Behzad Behdani:
Conceived and designed the analysis
Wrote the paper
Other contribution
Mohsen Tajdinian:
Conceived and designed the analysis
Contributed data or analysis tools
Wrote the paper
Marjan Popov:
Conceived and designed the analysis
Wrote the paper
Other contribution

Declarations of interest

We declare that there is no conflict of interest for this paper.

References

[1] H. Xue, M. Popov, Analysis of switching transient overvoltages in the power system of floating production storage and offloading vessel, Electr. Power Syst. Res. 115 (2014) 3–10.
[2] J. Kosmac, P. Zunko, A statistical vacuum circuit breaker model for simulation of transient overvoltages, IEEE Trans. Power Deliv. 10 (1) (1995) 294–300.
[3] L. Czarnecki, M. Lindmayer, Measurement and statistical simulation of multiple reignitions in vacuum switches, IEEE Trans. Plasma Sci. 13 (5) (1985) 304–310.
[4] N. Ueno, H. Toya, Y. Murai, M. Okada, Monte-Carlo simulation of overvoltage generation in the inductive current interruption by vacuum interrupters, IEEE Trans. Power Apparatus Syst. (3) (1984) 498–505.
[5] D.D. Shipp, T.J. Dionise, V. Lorch, B.G. MacFarlane, Transformer failure due to circuit-breaker-induced switching transients, IEEE Trans. Ind. Appl. 47 (2) (2011) 707–718.
[6] M. Popov, General approach for accurate resonance analysis in transformer windings, Electr. Power Syst. Res. 161 (2018) 45–51.
[7] B. Thomas, U. Savadamuthu, Impulse breakdown characteristics of aged oil impregnated paper, IEEE Trans. Dielectr. Electr. Insul. 24 (4) (2017) 2354–2361.
[8] T. Abdulahović, T. Thiringer, Voltage stress in a transformer winding during very fast transients caused by breaker closing event, IEEE Trans. Power Deliv. 29 (4) (2014) 1946–1954.
[9] W. Sima, P. Sun, Q. Yang, T. Yuan, C. Lu, M. Yang, Study on the accumulative effect of repeated lightning impulses on insulation characteristics of transformer oil impregnated paper, IEEE Trans. Dielectr. Electr. Insul. 21 (4) (2014) 1933–1941.
[10] T. Sels, et al., Effect of fast transients on distribution transformer insulation: switching transients modelling and material research, Proceedings of 17th International Conference and Exhibition on Electricity Distribution, CIRED 2003, 2003, p. 6 no. (1).
[11] E. Dullni, E. Lindell, L. Liljestrand, Dependence of the chopping current level of a vacuum interrupter on parallel capacitance, IEEE Trans. Plasma Sci. 45 (8) (2017) 2150–2156.
[12] T. Abdulahovic, T. Thiringer, M. Reza, H. Breder, Vacuum circuit-breaker parameter calculation and modelling for power system transient studies, IEEE Trans. Power Deliv. 32 (3) (2017) 1165–1172.
[13] B. Badrzadeh, M.H. Zamastil, N.K. Singh, H. Breder, K. Srivastava, M. Reza, Transients in wind power plants — part II: case studies, IEEE Trans. Ind. Appl. 48 (5) (2012) 1628–1638.
[14] N. Du, Y. Guan, J. Zhang, J. Niu, S. Yao, G. Xu, Phenomena and mechanism analysis on overvoltages caused by 40.5-kV vacuum circuit breakers switching off shunt reactors, IEEE Trans. Power Deliv. 26 (4) (2011) 2102–2110.
[15] Transformers-Switchgear-Committee, IEEE guide to describe the occurrence and mitigation of switching transients induced by transformers, switching device, and system interaction, number C57. 142, IEEE Power & Energy Society (2010).
[16] E.M. Hope, T.A. Bellei, M. Reyes, Wind turbine generator step-up transformer failure investigation, PES T&D 2012, IEEE, 2012, pp. 1–7.
[17] B. Badrzadeh, M. Hogdahl, E. Isabegovic, Transients in wind power plants — part I: modeling methodology and validation, IEEE Trans. Ind. Appl. 48 (2) (2012) 794–807.
[18] S. Ghafourian, I. Arana, J. Holbøll, T. Sørensen, M. Popov, V. Terzija, General analysis of vacuum circuit breaker switching overvoltages in offshore wind farms, IEEE Trans. Power Deliv. 31 (5) (2016) 2351–2359.
[19] Y. Xin, W. Tang, J. Zhou, Y. Yang, G. Liu, Sensitivity analysis of reignition overvoltage for vacuum circuit breaker in offshore wind farm using experiment-based modeling, Electr. Power Syst. Res. 172 (2019) 86–95.
[20] E. Lindell, L. Liljestrand, Effect of different types of overvoltage protective devices against vacuum circuit-breaker-induced transients in cable systems, IEEE Trans. Power Deliv. 31 (4) (2016) 1571–1579.
[21] D. Smugala, W. Piasecki, M. Ostrogorska, M. Florkowski, M. Fulczyk, O. Granhaug, Wind turbine transformers protection method against high-frequency transients, IEEE Trans. Power Deliv. 30 (2) (2015) 853–860.
[22] T. Abdulahovic, Analysis of High-Frequency Electrical Transients in Offshore Wind Parks, Chalmers University of Technology, 2011.
[23] C.L. Bak, et al., Vacuum circuit breaker modelling for the assessment of transient recovery voltages: application to various network configurations, Electr. Power Syst. Res. 156 (2018) 35–43.
[24] J. Lopez-Roldan, et al., Analysis, Simulation and Testing of Transformer Insulation Failures Related to Switching Transients Overvoltages, CIGRE, Paris, 2002, pp.

12–116.
[25] M. Popov, Switching Three-phase Distribution Transformers with a Vacuum Circuit Breaker: Analysis of Overvoltages and the Protection of the Equipment, Delft University of Technology, TU Delft, 2002.
[26] V. Hinrichsen, Metal-Oxide Surge Arresters in High-Voltage Power Systems, Fundamentals, Siemens AG, Erlangen, Germany, 2012.
[27] ABB documents, Surge Arrester MWK, (2013).
[28] J.A. Martinez-Velasco, Power System Transients: Parameter Determination, CRC press, 2017.
[29] E.C. Morgan, M. Lackner, R.M. Vogel, L.G. Baise, Probability distributions for offshore wind speeds, Energy Convers. Manage. 52 (1) (2011) 15–26.
[30] B. Kumaraswamy, B. Keshavan, Y. Ravikiran, Analysis of seasonal wind speed and wind power density distribution in aimangala wind form at chitradurga Karnataka using two parameter weibull distribution function, Power and Energy Society General Meeting, 2011 IEEE, IEEE, 2011, pp. 1–4.
[31] E. Zafeiratou, C. Spataru, R. Bleischwitz, Wind offshore energy in the Northern aegean Sea islanding region, environment and electrical engineering (EEEIC), 2016 IEEE 16th International Conference on, IEEE, 2016, pp. 1–7.
[32] J. Mahseredjian, G. Benmouyal, X. Lombard, M. Zouiti, B. Bressac, L. Gerin-Lajoie, A link between EMTP and MATLAB for user-defined modeling, IEEE Trans. Power Deliv. 13 (2) (1998) 667–674.
[33] A. Theocharis, M. Popov, R. Seibold, S. Voss, M. Eiselt, Analysis of switching effects of vacuum circuit breaker on dry-type foil-winding transformers validated by experiments, IEEE Trans. Power Deliv. 30 (1) (2014) 351–359.
[34] P.E. Sutherland, M.E. Valdes, G.H. Fox, Snubber design for transformer protection, IEEE Trans. Ind. Appl. 52 (1) (2016) 692–700.